



## RESIDUAL AXIAL BEHAVIOR OF FIRE-DAMAGED REINFORCED CONCRETE COLUMNS

M. Monir A. Alhadid (MAA)  
PhD Candidate, Canada

Maged A. Youssef (MA)  
Professor, P.Eng., Canada

### ABSTRACT

Engineers need a simplified procedure to predict the residual axial capacity and stiffness of Reinforced Concrete (RC) columns exposed to a complete heating-cooling cycle. Finite difference heat transfer and sectional analysis models are developed to determine the axial behavior of such columns with various end-restraint conditions at different fire durations. The influence of cooling phase on temperature distribution and residual mechanical properties are considered in the analysis. The ability of the model to predict the axial behavior of the damaged columns is validated in view of related experimental studies and shown to be in very good agreement. A parametric study is then conducted to assess the axial performance of fire-damaged RC columns. A procedure is proposed to determine the residual strength and stiffness of fire-damaged RC columns in typical frame structures.

Keywords: - Reinforced Concrete; Residual; Fire; Temperature; Restraints.

### 1. INTRODUCTION

The fire incident data published by the Council of Canadian Fire Marshals and Fire Commissioners showed that a total of 42,753 fire incidents occurred in the Canadian provinces in 2007 alone resulting in 224 civilian deaths and CAD \$ 1,551,657,179 direct property damage (Wijayasinghe 2011). With such high figures, it is mandatory to develop a procedure to assess the residual performance of the structural system after fire. Most concrete structures exposed to fire conditions are not fully deteriorated and their structural integrity and mechanical properties can be restored by applying suitable repair methods (ACI 201.1R 2008). In the current design practice, a preliminary assessment of the damaged members is performed immediately after being exposed to elevated temperatures by inspecting the building. Both visual inspection and hammer tapping techniques are carried out to identify the maximum temperature reached, fire propagation route, residual strength of concrete, cracking schemes, color changes and smoke characteristics. After that, the structure is evaluated and repaired according to the relevant design code depending on the extent of damage and the affordability of the required work (Concrete Society 2008).

Although considering the temperature and load history experienced by the structural members is of great importance, the current design codes overlook providing a detailed examination in the relevant clauses. In an extensive fire-related study performed by Anderberg (1976), it was stated that "*Concrete has memory*" to indicate the significant influence of temperature-load interaction on the residual behavior of fire-damaged members. In the current study, the temperature and load history acting on various RC members in typical RC structures is taken into account to assess their residual structural behavior. The various strain components developed during and after fire are calculated and their influence on changing the residual performance of the damaged members under various restraining conditions is evaluated. The impact of varying the geometrical and mechanical properties of the exposed members as well as the influence of fire duration on their residual structural integrity are examined. The proposed analytical model is validated against relevant experimental studies. An extensive parametric investigation is then carried out to propose a robust yet simple procedure for engineers to accurately assess the residual performance of fire-damaged members. The outcomes of the current study is an important milestone towards incorporating the performance-based approach into standards and regulations.

## 2. ANALYSIS APPROACH

An accurate assessment of post-fire behavior of RC members in typical frame structures requires the consideration of (1) the residual mechanical properties of the composing materials; and (2) the temperature-load interaction before and during fire. In order to achieve both criteria, the analytical approach, performed in this study, encompasses three main stages that describe the structural variations in the exposed member throughout the heating-cooling cycle. Firstly, the structural performance of the intact member is determined in terms of its capacity and stiffness considering the relevant material models at ambient conditions. The obtained structural characteristics act as a basis to calculate the initial load level ( $\lambda$ ) and to determine the extent of deterioration in the member after fire exposure. The second stage involves thermal and structural analyses of the exposed member during the heating and cooling cycles. Heat transfer analysis is carried out using the finite difference method in order to determine the maximum temperature distribution within the member depending on concrete thermal and physical properties. The residual properties of the member at the final stage (point 2) is highly dependent on the temperature-stress path followed as indicated in Fig.1(a). Therefore, at each time increment, the change in the applied load level is also calculated based on the additional restraint forces. Both thermal and transient strains are calculated at each time increment at the corresponding temperature-stress combination represented by the stepped curve in Fig.1(a). In addition, the residual capacity of the member during fire is calculated based on the relevant material models to ensure that failure is not reached. The third analysis stage initiates after the member is completely cooled down to room temperature. In this stage, sectional analysis is carried out to determine the residual capacity and stiffness of the fire-damaged member depending on the recorded data including the maximum temperature reached and residual strain distribution. The analysis is performed by applying uniform strain increments until failure occurs taking into account related post-fire mechanical properties and material models.

The current study focuses on the axial behavior of rectangular RC members exposed to fire from all sides. The geometrical properties and reinforcement distribution of a typical cross-section considered in the analysis are defined in Fig.1(b) in terms of section width ( $b$ ), section height ( $h$ ), concrete cover, top steel reinforcement ( $A_{st}$ ) and bottom steel reinforcement ( $A_{sb}$ ). To account for the restraint conditions, a pin support is assigned to one end of the member, while the other end is attached to a roller support and a spring having an axial stiffness of ( $k_{\delta}$ ) as illustrated in Fig.1(c). Spring stiffness represents the axial constraints provided by the adjacent beams and columns in an actual frame structure and can be obtained with the aid of any commercially available software for structural analysis. While the spring is considered to resist the expansion tendency of the member, it does not affect any possible contraction the member may experience.

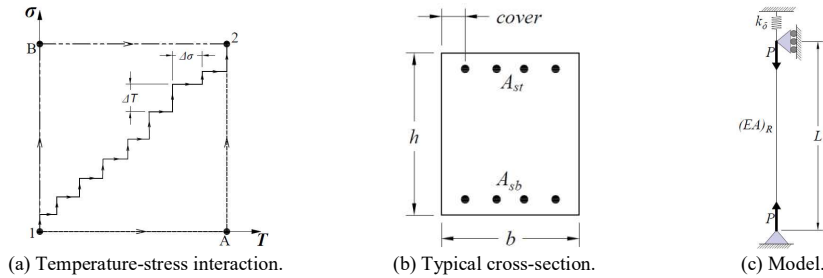


Figure 1: Main considerations in the proposed analytical analysis.

## 3. ASSUMPTIONS

The proposed analytical model is performed considering the following assumptions: (1) a cross section remains plane before, during, and after fire exposure, (2) perfect bond exists between steel reinforcement and the surrounding concrete material, (3) spalling of concrete is neglected in the analysis, (4) two dimensional heat transfer analysis is considered in the member, (5) influence of concrete tensile cracks on heat flow is neglected in heat transfer analysis, (6) the only source of nonlinearity in the analysis arises from materials behavior, whereas geometrical nonlinearity is not considered. (7) failure of the member is not governed by buckling.

#### 4. THERMAL ANALYSIS

Temperature distribution at any section along the member is determined based on the finite difference method described by Lie (1992) and validated with relevant experimental data by Alhadid and Youssef (2016). The analysis procedure begins by dividing the cross section into multiple elements as shown in Fig. 2 (a). The point at the center of each internal element or on the hypotenuse of each boundary element represents the temperature of the entire element. Steel bars are considered as perfect conductors due to their high thermal conductivity and their temperature is assumed to be identical to the adjacent concrete elements. The physical and thermal properties of both concrete and steel are provided by Lie (1992). For each time increment, temperature distribution within the section is obtained by solving the heat balance equations of all elements. In the current study, the member is exposed to an ASTM E119 (2001) standard fire along its perimeter during the heating phase as given by Equation 1.

$$[1] T_f - T_o = 750 [1 - e^{(-3.79553 \sqrt{t})}] + 170.41\sqrt{t}$$

where  $T_f$  is the fire temperature ( $^{\circ}\text{C}$ ),  $T_o$  is the room temperature ( $^{\circ}\text{C}$ ) and  $t$  is the time after the start of the fire (hr). During the cooling phase, temperature is assumed to decrease gradually according to ISO 834 (2014) specifications in terms of fire duration since the ASTM E119 (2001) standards do not provide a descending branch. Concrete thermal properties are assumed to be irreversible and maintain a constant value corresponding to the maximum temperature reached (Schneider 1985, Hertz 2005). Figure 2 (b) illustrates the change in temperature at different points within a rectangular  $400 \text{ mm} \times 500 \text{ mm}$  section exposed to fire from all sides for 1.5 hrs followed by a cooling phase. Three main observations can be drawn from this figure: (1) the points closer to the surface respond faster to the variation in the fire time-temperature curve than the interior points, (2) the maximum temperature in the interior elements is reached during the cooling phase indicating that heat flow propagates not only to the atmosphere, but also to the inner colder portions of the member, (3) the cooling continues for a considerable amount of time before heat flow takes one direction only toward the atmosphere. Figure 2(c) shows the maximum temperature distribution within the aforementioned cross section after a complete heating-cooling cycle. This distribution results in higher temperature values than that at the end of the heating phase. The residual mechanical properties and constitutive relationships of both concrete and steel are determined in the following sections based on the maximum temperature reached.

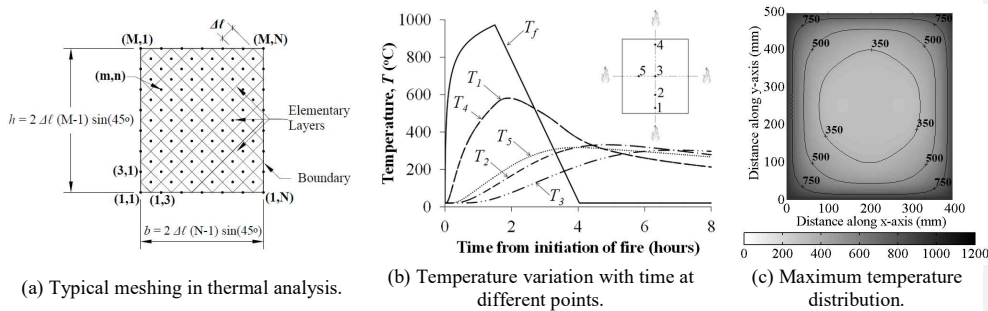


Figure 2: Determination of temperature distribution within a typical rectangular cross-section.

#### 5. MATERIAL MODELS AND STRAIN COMPONENTS

The general form of Tsai (1988) model is adopted to represent the compressive stress-strain relationship of concrete at all stages. During fire, the reduced compressive strength due to fire ( $f'_{cr}$ ) proposed by Hertz (2005) is adopted; whereas, concrete strain at peak stress at elevated temperatures ( $\epsilon_{oT}$ ) is determined by Terro (1998) formula. The post-fire mechanical properties are calculated based on the expressions provided by Chang *et al.* (2006).

Regarding steel constitutive models, Karthik and Mander (2011) model is adopted for both ambient and post-fire conditions as it conveniently combines the initial elastic response, yield plateau and strain hardening stages in a rigorous form. At elevated temperatures, Lie (2004) model is used as it implicitly includes the reduction in yield strength due to fire. The post-fire mechanical properties of steel are obtained from the expressions proposed and validated by Alhadid and Youssef (2016).

Total strain in concrete ( $\epsilon$ ) is calculated as the summation of stress-related strain ( $\epsilon_\sigma$ ), free thermal strain ( $\epsilon_{th}$ ), creep strain ( $\epsilon_{cr}$ ), and transient strain ( $\epsilon_{tr}$ ). The deformation tendency of structural members due to external applied loads is described in terms of the stress related strain. Free thermal strain of both concrete and steel bars is determined from EN 1992-1-2 (Eurocode 2004) proposed expressions. Regarding the transient and creep strains, the empirical model proposed by Terro (1998) is adopted as it determines the value of both strain components simultaneously as referred to by load induced thermal strain ( $\epsilon_{LITS}$ ).

## 6. STRENGTH ANALYSIS

An iterative sectional analysis procedure is carried out to determine the residual  $P-\epsilon$  behavior of the fire-damaged RC columns. At every loading step, the axial strain is increased incrementally until reaching the total applied axial load. The kinematic and compatibility conditions are considered in view of the corresponding residual mechanical properties and stress-strain relationships of both concrete and steel. To maintain the high accuracy while reducing the computation time, a sensitivity analysis was performed and the maximum layer height is chosen as not to exceed 2 mm. The failure criterion of the RC element is defined by crushing of concrete once the strain in any of the sectional layers reaches the residual ultimate strain ( $\epsilon_{cuR}$ ) proposed and validated by Alhadid and Youssef (2016).

Figures 3(b) through 3(e) illustrate the development of the strain components along section (A-A) in Figure 3(a). The residual free thermal strain ( $\epsilon_{thR}$ ) represents the irreversible part of the free expansion that occurred during fire. The reduction rate in concrete thermal strain is taken as  $8 \times 10^{-6} / ^\circ\text{C}$  (Guo and Shi 2011), while  $\epsilon_{thR}$  for steel is set to zero. If the member is initially loaded, then transient strain is generated in concrete and maintains its maximum values after cooling (Guo and Shi 2011). The difference between the residual thermal strain ( $\epsilon_{thR}$ ) and the residual transient strain ( $\epsilon_{trR}$ ) is the total residual strain ( $\epsilon_R$ ) which can be either positive or negative depending on the temperature-load history. Residual stress-induced strain ( $\epsilon_{\sigma i}$ ) distribution is determined as the difference between an equivalent strain ( $\epsilon_{eq}$ ) and the total residual strain ( $\epsilon_R$ ).

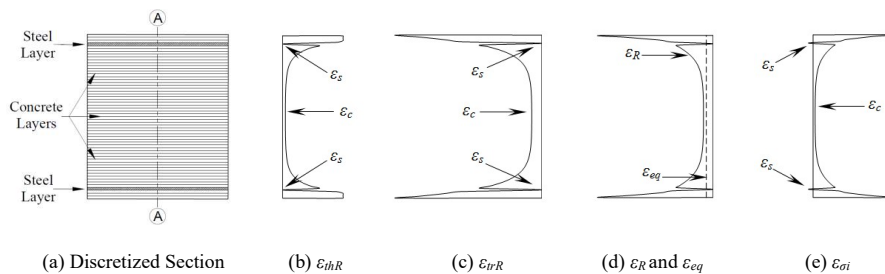


Figure 3: Development of various strain components along the discretized cross-section.

Residual stresses are induced in fire-damaged members for two main reasons: (1) thermal strain in concrete is partially reversible, while transient strain is completely irreversible (Guo and Shi 2011). At equilibrium, unloaded fire-damaged concrete tends to remain either expanded or contracted after fire depending on the temperature-load history. On the other hand, thermal strain in steel is fully reversible, while transient strain does not develop. Hence, steel bars tend to restore their initial length after fire. The variation in behavior between concrete and the embedded steel bars generate internal stresses to achieve equilibrium. (2) both thermal and transient strain distributions along section height are nonlinear as they follow the nonlinear temperature profile. Therefore, internal stresses are

developed in order to maintain the plane section assumption. An iteration process is performed by changing the  $\epsilon_{eq}$  and checking the equilibrium condition of  $\epsilon_{si}$  distribution. Once equilibrium is achieved,  $\epsilon_{si}$  are applied as initial strains in the concrete and steel layers; whereas,  $\epsilon_{eq}$  results in shifting the  $P-\epsilon$  curve as illustrated in Figure 4(a). Unloaded members tend to expand when heated, resulting in expansion  $\epsilon_{eq}$  to achieve equilibrium as shown in Fig. 4(b). However, if the member is loaded when exposed to heat, then it contracts due to the influence of transient strain. Therefore, the contraction to the entire member after cooling as indicated by  $\epsilon_{eq}$  in Fig. 4(c).

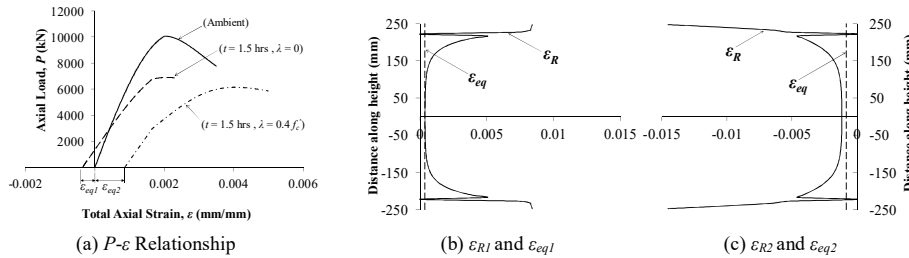


Figure 4: Influence of initial load level on the residual ( $P-\epsilon$ ) relationship and residual strain distribution.

## 7. VALIDATION OF THE PROPOSED MODEL

The capability of the present model to predict the post-fire structural performance of axially loaded RC members is validated in view of the experimental results obtained by Chen *et al.* (2009) and Jau and Huang (2008). The validation is limited to structural members made of normal strength concrete where spalling does not occur.

### 6.1 Chen *et al.* (2009)

Chen *et al.* (2009) carried out full-scale experiment to investigate the performance of RC columns after exposure to different fire conditions. The results obtained from the proposed analytical model are compared with the measured data of columns FC06 and FC05. These columns are exposed to ISO 834 (2014) standard fire curve from four sides for 2 hrs and 4 hrs, respectively. The tested columns have cross-sectional dimensions of 300 mm  $\times$  450 mm, concrete cover of 40 mm and overall length of 3.0 m. The concrete compressive strength at ambient conditions is 29.5 MPa. The longitudinal reinforcement consists of 4 $\Phi$ 19 mm and 4 $\Phi$ 16 mm steel bars having yield strengths of 476 MPa and 479 MPa, respectively. Both columns were subjected to an initial axial load of 797 kN prior to heat exposure. After 30 days from the fire test, the columns were subjected to the constant initial concentric load of 797 kN while another eccentric load is applied until failure. Fig. 5(a) shows the analytical and experimental load-deflection curves at the column mid-span due to the eccentric load about the y-axis for columns FC06 and FC05 corresponding to fire duration of 2 and 4 hours, respectively. A very good agreement between both curves can be shown with a percent difference of 3.8% and 4.6% in the ultimate capacity of columns FC06 and FC05, respectively; and a percent difference of 6.3% and 5.4% in the 40% secant stiffness for the same two columns, respectively. This variation can be attributed to the sensitivity of the adopted thermal expansion model to the experimental conditions and concrete mix that it was derived from. Also, the heating-cooling cycle adopted in the model follows the ISO 834 provisions which may be different from the actual relationship followed in lab.

### 6.2 Jau and Huang (2008)

In another experimental study, Jau and Huang (2008) investigated the residual behavior of initially loaded restrained RC columns subjected to heat from two adjacent sides. The cross-sectional dimensions of all columns are 300 mm  $\times$  450 mm with an overall length of 2.7 m. The concrete cover varies between 50 mm or 70 mm, whereas the steel reinforcement ratio varies between 1.8% and 3.0%. Normal strength concrete with compressive strength of 33.7 MPa and steel bars with yield strength of 475.8 MPa are used. The test setup allows the heat to flow through two adjacent surfaces only while the other two surfaces are insulated and not subjected to fire. The restrained columns are subjected to a 10% axial preloading of their ambient compressive strength during the 2 or 4 hours fire test. After the columns naturally cooled down, the load is applied until failure occurs. Figure 5(b) shows both the experimental

and predicted residual capacity of columns A12, B12, A14, A24 and B24 whose detailed geometrical and mechanical properties are provided by Jau and Huang (2008). The proposed model is found to predict the capacity of the tested columns with high accuracy as indicated by the maximum percent error of 5.3% depicted of column A14 shown in the figure. Overall, the agreement between the experimental and analytical results is very good.

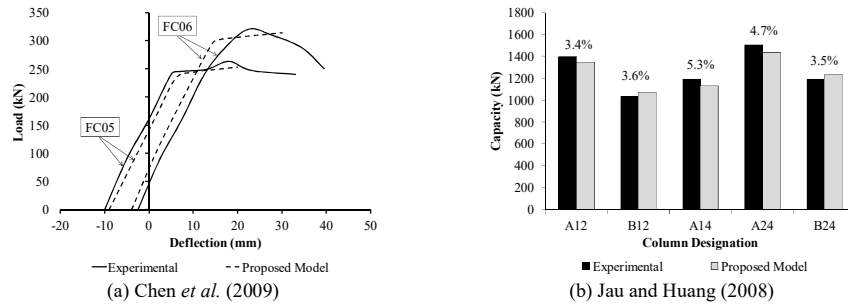


Figure 5: Validation of the proposed analytical model with experimental data.

## 8. PARAMETRIC STUDY

The influence of the considered parameters on the post-fire behavior of rectangular RC columns is investigated in view of an extensive parametric study. The members are exposed to ASTM E119 (2001) standard fire along their perimeters followed by a cooling phase as described in section 4. The main parameters include the concrete compressive strength,  $f'_c$  (25 MPa and 35 MPa); steel yield strength,  $f_y$  (300 MPa and 400 MPa); member height,  $h$  (400 mm and 800 mm); member width,  $b$  (300 mm and 600 mm); fire duration,  $t$  (0.5 hr, 1.5 hrs and 2.5 hrs); initial load level,  $\lambda$  (0.0,  $0.2 f'_c$ ,  $0.4 f'_c$ ); axial restraint stiffness,  $R_\delta$  (0.0, 0.5 and 1.0); and steel reinforcement ratio,  $\rho$  (0.02 and 0.04). Concrete cover is taken as 30 mm from the bar centroid to the nearest concrete surface. Based on these parameters, the analytical investigation consists of a total of 864 different cases.

The effect of the aforementioned parameters on both the residual axial capacity ( $P_R$ ) and the residual 40% secant axial stiffness ( $EA_R$ ) is determined in view of the members presented in Table 1. The variation of these two characteristic behaviors as functions of the different parameters are shown in Figs. 6(a) through 6(f) at different load levels. The Reduction Ratio in these figures is defined as the proportion of the residual capacity (or stiffness) to its counterpart at ambient conditions.

Table 1: Properties of the examined sections.

Case	$t$ (hr)	$f'_c$ (MPa)	$f_y$ (Mpa)	$b$ (m)	$h$ (m)	$\rho$	$R_\delta$
R1	1.5	35	400	400	500	0.04	0.0
R2	0.5	35	400	400	500	0.04	0.0
R3	2.5	35	400	400	500	0.04	0.0
R4	1.5	25	400	400	500	0.04	0.0
R5	1.5	35	300	400	500	0.04	0.0
R6	1.5	35	400	250	500	0.04	0.0
R7	1.5	35	400	600	500	0.04	0.0
R8	1.5	35	400	400	300	0.04	0.0
R9	1.5	35	400	400	800	0.04	0.0
R10	1.5	35	400	400	500	0.02	0.0
R11	1.5	35	400	400	500	0.04	0.5
R12	1.5	35	400	400	500	0.04	1.0

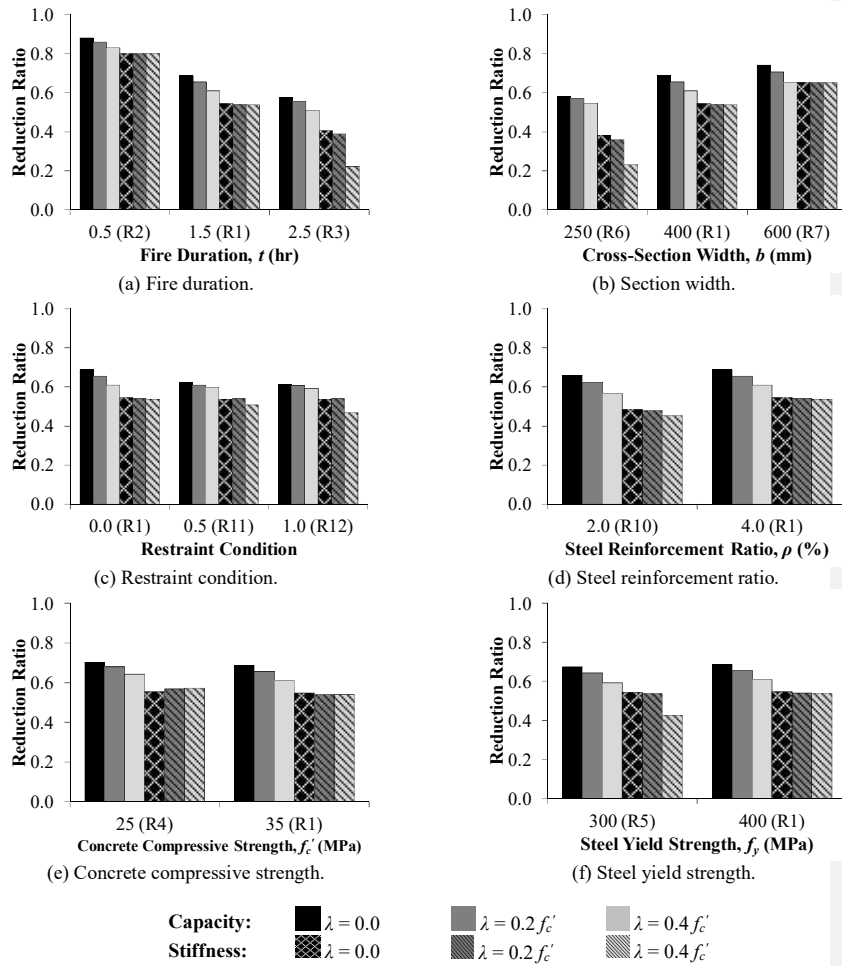


Figure 6: Influence of varying the examined parameters on the residual axial capacity and stiffness.

### 8.1 Effect of Fire Duration ( $t$ )

Fire duration is found to have the most significant influence on reducing the post-fire capacity and stiffness of RC columns. Figure 6(a) indicates that increasing the fire duration from 0.5 hr to 2.5 hrs causes an additional 30% drop in the capacity reduction ratio and an extra 41% in stiffness reduction ratio for all columns regardless of the initial load level. This is justified by the additional deterioration in both concrete and steel residual mechanical properties caused by the longer duration of the heating-cooling cycle which provides more time for heat to transfer to the inner elementary layers raising their temperatures.

## 8.2 Effect of Section Size

Increasing the width of the cross-section results in higher residual flexural strength and stiffness after fire as indicated in Fig. 6(b). This larger residual capacity is caused by the lower temperature increase within the wider member as it requires more heat energy to increase its temperature. For the same fire duration, concrete within the inner parts of the wider member experience lower increase in temperature and consequently more recovery after fire. The influence of strength recovery in steel bars is neglected since concrete cover is the same in all specimens causing the maximum temperature reached in all steel bars to be the same. The same influence is determined for increasing the section height for the same aforementioned reason. In addition, increasing section height shifts the concrete core away from the corners where the maximum temperature condensation exists resulting in reducing concrete degradation after fire.

## 8.4 Effect of Restraint Conditions

The influence of restraining the member against thermal expansion during heating is found to slightly increase its post-fire stiffness and capacity as shown in Fig. 6(c). This is explained by knowing that transient strain component significantly alleviates the extent of thermal expansion, which means that the overall thermal expansion pushing the stiffer supports is smaller than that exerted on unrestrained supports. Thus, the additional restraint axial forces developed in the restrained members are not very large to significantly alter its residual capacity. The change in the generated restraint load is characterized by a mild increase followed by a gradual degradation with time. In the first stage, the member's stiffness remains close to that at ambient conditions as the temperature increase within the member is relatively low. Thus, an increase in restraining force is observed to hinder the higher thermal expansion tendency exhibited by the member. However, after certain period of time, the temperature within the member becomes relatively high causing the stiffness degradation to become more pronounced. Thus, the forces required to resist the larger thermal expansion of the member drops.

## 8.5 Effect of Steel Reinforcement Ratio

Increasing the steel reinforcement ratio is shown to have a negative impact on the residual capacity and stiffness of fire-damaged members as indicated in Fig. 6(d). For instance, increasing  $\rho$  from 0.02 to 0.04 results in a consequent increase in the reduction ratio by about 5% and 14% for capacity and stiffness, respectively. This insignificant decrease is attributed to the higher impact of the larger steel area in representing the permanent deterioration steel bars' yield strength and modulus of elasticity after fire.

## 8.3 Effect of Mechanical Properties

Increasing the concrete compressive strength is found to have an insignificant inverse relationship on the reduction ratio of both capacity and stiffness for all load levels in the examined range as shown in Fig. 6(e). The decreasing rate can be justified by the more reduction in compressive strength of the stronger concrete after fire. Hence, the reduction in concrete contribution within the compression zone becomes more pronounced and results in the observed larger decrease relative to the original capacity. The use of normal strength concrete infers that no spalling is encountered which could otherwise significantly affect the residual capacity.

Regarding the steel yield strength, increasing the grade from 300 MPa to 400 MPa results in a further reduction in the residual capacity and stiffness as indicated by the 4.3% and 6.8% increase, respectively. The reason for this observation lies in the more pronounced reduction in residual yield strength for the steel bars of higher grade as described by the material models.

## 8.5 Effect of Initial Load Level

A comparison of the examined members reveals that increasing the applied load level causes a reduction in the reduction ratio. For example, applying a  $0.4 f_c'$  initial load level decreases the residual strength by about 9.3% in column R10 relative to its unloaded condition as indicated in Fig. 13(d). This is caused by the larger applied strain at the end of the heating phase and the lower residual concrete strength in the compression zone. Hence, concrete crushing occurs at lower axial load than the case of unloaded members. This change in behavior is attributed to the transient and creep strains that possess a counteractive influence on the member's response to elevated temperatures.

Formatted: Paragraph, Space After: 0 pt, Line spacing: single



## 9. PROPOSED SIMPLIFIED EQUATIONS

Accurate determination of temperature distribution and residual strain components developed within RC columns is tedious and requires detailed thermal and structural analyses that may not be convenient for design engineers. Hence, based on the extensive parametric study conducted on 864 different cases, regression analysis is carried out to develop expressions for obtaining both the residual axial capacity and residual 40% secant axial stiffness of fire-damaged RC columns. These proposed expressions take into consideration the loading history, restraint conditions, fire duration, geometrical properties and mechanical properties of the exposed members. The validity and accuracy of the proposed equations depend on the range of parameters considered in the parametric study.

### 8.1 Axial Capacity

The residual axial capacity ( $P_R$ ) is calculated by multiplying the intact column's capacity by the ratio ( $\alpha_p$ ) given in the proposed Equation 3.

$$[3] \alpha_p = 0.641 + 0.0541 t^2 - 0.311 t + 0.00514 \frac{f_y}{f_c} + 0.254 b + 0.219 h + 1.92 \rho - 0.0967 \lambda - 0.0374 R_D$$

where  $\alpha_p$  is the axial capacity reduction ratio,  $t$  is the fire duration at the end of the heating phase (hr),  $f_y$  is the steel yield strength (MPa),  $f_c$  is the concrete compressive strength (MPa),  $b$  is section width (m),  $h$  is section height (m),  $\rho$  is steel reinforcement ratio,  $\lambda$  is the initial load level relative to ambient capacity, and  $R_D$  is the axial restraint ratio. Figure 7(a) shows a very good agreement between the values predicted from Equation 3 and the results determined through performing detailed analytical analysis for all examined cases.

### 8.2 Axial Stiffness

The 40% secant axial stiffness ( $EA_R$ ) is determined by multiplying the corresponding axial stiffness at ambient conditions with the ratio ( $\alpha_{EA}$ ) calculated from the proposed Equations 4 and 5.

$$[4] \alpha_{EA} = -0.7824 R_{EA}^2 + 1.8842 R_{EA} - 0.2024$$

$$[5] R_{EA} = 0.413 + 0.0823 t^2 - 0.481 t + 0.00734 \frac{f_y}{f_c} + 0.709 b + 0.247 h + 3.16 \rho - 0.161 \lambda - 0.0345 R_D$$

where  $\alpha_{EA}$  is the stiffness reduction ratio, and  $R_{EA}$  is a factor calculated in terms of all considered parameters. The expectation function of the proposed ratio is determined considering nonlinear regression analysis of the data. The line of equality plot reveals that the model provides an excellent prediction of the actual behavior. The presence of outliers is almost negligible which enhances the confidence of using the proposed expressions.

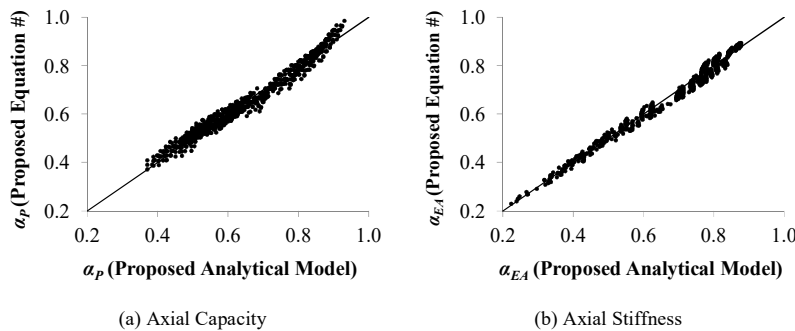


Figure 7: Validation of the proposed equations with the proposed model results.

## 10. CONCLUSIONS

In this paper, both thermal and sectional analyses are performed aiming at determining the residual behavior of fire-damaged members in typical RC frames. The temperature-load history experienced by the exposed members is considered in detail in the analytical study. The model is validated against relevant experimental studies and a parametric study is then carried out to determine the influence of various loading conditions and fire scenarios on the residual properties of the members. The study has led to developing a performance-based method to allow engineers evaluate the deterioration in fire-damaged members and to assess the extent of repair required after the fire incident. Main findings coming out of this study are as follow: (1) fire duration and member width have the most significant influence on the residual stiffness and capacity of the fire-damaged members, (2) The initial load level has minor impact on the residual flexural strength ratio of fire-damaged members, (3) Subjecting a member to a moderate initial load before and during heating, both transient and creep strains are developed and counteract thermal expansion tendency of the member, (4) Increasing the concrete compressive strength and steel grade is found to have an insignificant impact on the reduction in the residual flexural capacity of the fire-damaged member for all load levels in the examined range.

## 11. REFERENCES

- ACI Committee 201. 2008. *Guide for Conducting a Visual Inspection of Concrete in Service*, American Concrete Institute, Farmington Hills, MI, USA.
- Alhadid, MM, Youssef, MA. 2016. A Simplified Method to Calculate the Flexural Capacity of Fire-Damaged Reinforced Concrete Beams. (In Progress).
- Anderberg, Y. 1976. *Stress and Deformation Characteristics of Concrete at High Temperatures*, Lund Institute of Technology, Stockholm, Sweden.
- ASTM. 2001. *Standard Methods of Fire Test of Building Construction and Materials, Test Method E119-01*, American Society for Testing and Materials, West Conshohocken, PA, USA.
- Chang, Y.F., Chen, Y.H., Sheu, M.S., and Yao, G.C. 2006. Residual Stress-Strain Relationship for Concrete after Exposure to High Temperatures. *Cement and Concrete Research*, 36 (10): 1999-2005.
- Chen, Y.H., Chang, Y.F., Yao, G.C., and Sheu, M.S. 2009. Experimental Research on Post-Fire Behaviour of Reinforced Concrete Columns. *Fire Safety Journal*, 44 (5): 741-748.
- Concrete Society. 2008. *Assessment, Design and Repair of Fire-Damaged Concrete Structures*, The Concrete Society, Camberley, UK.
- EN 1992-1-2. 2004. *Eurocode 2: Design of Concrete Structures - Part 1-2: General Rules - Structural Fire Design*, European Committee for Standardization.
- Guo, Z. and Shi, X. 2011. *Experimental and Calculation of Reinforced Concrete at Elevated Temperatures*. Butterworth-Heinemann, Oxford, UK.
- Hertz, K.D. 2005. Concrete Strength for Fire Safety Design. *Magazine of Concrete Research*, 57 (8): 445-453.
- ISO. 2014. *Fire Resistance Tests, Elements of Building Construction, ISO 834-11*, International Organization for Standardization, London, UK.
- Jau, W.C. and Huang, K.L. 2008. A study of reinforced concrete corner columns after fire. *Cement Concrete Composites*, 30 (7): 622-638.
- Karthik M., and Mander J. 2011. Stress-block parameters for unconfined and confined concrete based on a unified stress-strain model. *Journal of Structural Engineering*, 137 (2): 270-273.
- Lie, T.T. 1992. *Structural Fire Protection*, ASCE Manuals and Reports on Engineering Practice, No. 78, New York, NY, USA.
- Schneider, U. 1985. *Properties of Materials at High Temperatures: Concrete*, RILEM, Kassel, Germany.
- Terro, M.J. 1998. Numerical modeling of the behavior of concrete structures in fire. *ACI Structural Journal*, 95 (2): 183-93.
- Tsai, W.T. 1988. Uniaxial Compressional Stress-Strain Relation of Concrete. *Journal of Structural Engineering*, 114 (9): 2133-2136.
- Wijayasinghe, M. 2011. *Fire Losses in Canada*, Association of Canadian Fire Marshals and Fire Commissioners, Calgary, Alberta, Canada.